Fracturing Spacing Optimization Study of Tight Oil Horizontal Well Based on Induced Stress Field

Jia-wei Ren[1,2(✉)], Qi-hong Feng[1,2], Xian-min Zhang[1,2], and Ze-hao Xie[1,2]

[1] School of Petroleum Engineering, China University of Petroleum (East China), Qingdao, Shandong, China
[2] Key Laboratory of Unconventional Oil & Gas Development (China University of Petroleum (East China)), Ministry of Education, Qingdao, Shandong, China

Abstract. Tight oil reservoirs in the Songliao Basin have characteristics such as poor permeability parameters and undeveloped natural fractures. Reducing the fractural spacing and subdivision cutting the reservoir is to explore the trend and direction of enhancing SRV and recovery. This paper analyzes the induced stress field during the fracture propagation process of horizontal well tight cutting, and then uses XFEM numerical simulation method to study the optimization of fracture spacing. The results show that with the increase of the distance from the fracture, the induced stress difference caused by the pre-fracture in the horizontal well increases first and then decreases. In the effective range where the induced stress difference is greater than 0, turning or even reversal occurs when a new fracture is propagated. Define the corresponding position when the induced stress difference equals the initial geostress field difference as the minimum cluster spacing ΔL_{min}. During the fracturing construction, arranging fractures larger than ΔL_{min} can ensure that the cluster spacing is as small as possible and also allow the fractures to expand normally. As a result, multiple parallel effective main fractures are formed to achieve dense cutting of tight oil reservoirs, thereby increasing the SRV. This conclusion can be used as reference for the optimization design of subdivision cutting and fracturing spacing in Daqing Oilfield and other tight oil reservoirs in the future.

Keywords: Induced stress field · Horizontal well · Subdivision cutting · Fracture spacing

1 Introduction

At present, tight reservoirs have become an important part of oil and gas resources, with characteristics of poor reservoir physical properties and poor continuity. Volumetric fracturing of long horizontal wells is one of the efficient development methods for tight reservoirs [1–3]. The focus of traditional volume fracturing is the formation of complex fracture grids, that is, the main fracture communicates with micro-fractures such as natural fractures to form complex fractures, thereby expanding the contact area between the matrix and fractures, and increasing the SRV [4–6]. However, for the

Daqing tight oil reservoir, natural fractures are basically not developed, Therefore, the conditions for forming complex cracks are not available, and the artificial fracture are mainly Bi-wing fracture. For a long time, Daqing Oilfield has achieved good development results by using horizontal wells and multi-cluster fracturing technology [7, 8].

Reservoir dynamic evaluation data show that when the cluster spacing is too large, there is unused area between the fractures and fractures; therefore, reducing the cluster spacing to achieve dense cutting of the reservoir is an effective way to increase the volume of the reservoir reconstruction. There are problems such as stress interference and economic cost at the same time [9–12]. At present, scholars at home and abroad focus on the optimization of cluster spacing, mainly using reservoir numerical methods, with production or economy as the optimization target, without considering the influence of stress interference on fracture propagation [13, 14]. During the fracturing construction of horizontal wells, since the fractures cannot be synchronized, the induced stress field generated by the first fracture can affect or even prevent the expansion and extension of the later fractures [15]. Therefore, the cluster spacing needs to be scientifically calculated. Too large or too small are not consistent with actual production conditions. In view of this, the author aims to pursue the minimum cluster spacing to maximize the volume of reservoir reconstruction. The numerical simulation method is used to analyze the induced stress field generated by the first compression fracture. Then, by comparing the relationship between the induced stress difference and the initial horizontal ground stress difference, the principle of determining the minimum cluster spacing is proposed to optimize the fracture spacing.
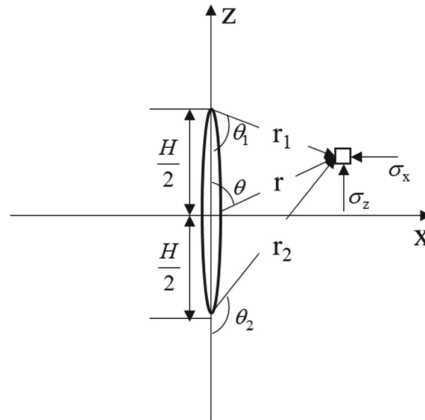
2   Methodology

2.1   Hydraulic Fracture Induced Stress Field

A large number of studies have shown that hydraulic fracturing fractures generate induced stress fields around them, and new fracturing fractures will be disturbed by the stress of pre-fractured fractures, and there will be compound stress interference between multiple fractures. Based on elastoplastic mechanics theory, a geometric model is established. The model selects the two-dimensional plane where the fracture height is located to analyze the induced stress field of the fracture. The horizontal minimum principal stress direction is taken as the X axis, and the horizontal maximum principal stress Z axis is used to establish a coordinate system (Fig. 1).

According to Sneddon's analytical solution [16–18], the formula for calculating the stress induced by two-dimensional vertical fracture can be obtained as follows:

$$\sigma_{xi} = p\frac{r}{c}(\frac{c^2}{r_1 r_2})^{\frac{3}{2}}\sin\theta \cdot \sin\frac{3}{2}(\theta_1 + \theta_2) + p\left[\frac{r}{(r_1 r_2)^{\frac{1}{2}}}\cos\left(\theta - \frac{1}{2}\theta_1 - \frac{1}{2}\theta_2\right) - 1\right] \quad (1)$$

$$\sigma_{zi} = -p\frac{r}{c}(\frac{c^2}{r_1 r_2})^{\frac{3}{2}}\sin\theta \cdot \sin\frac{3}{2}(\theta_1 + \theta_2) + p\left[\frac{r}{(r_1 r_2)^{\frac{1}{2}}}\cos\left(\theta - \frac{1}{2}\theta_1 - \frac{1}{2}\theta_2\right) - 1\right] \quad (2)$$

Fig. 1. A figure caption is two-dimensional vertical fracture induced stress field

According to Hook's law:

$$\sigma_{yi} = v(\sigma_{xi} + \sigma_{yi}) \tag{3}$$

$$\tau_{xzi} = p\frac{r}{c}\left(\frac{c^2}{r_1 r_2}\right)^{\frac{3}{2}} \sin\theta \cdot \cos\frac{3}{2}(\theta_1 + \theta_2) \tag{4}$$

In the formula, p is the net pressure in the fracture, H is the fracture height, $c = H/2$, and the following mathematical relationships exist for each geometric parameter:

$$r = \sqrt{x^2 + y^2}, \quad \theta = \arctan(x/y) \tag{5}$$

$$r_1 = \sqrt{x^2 + (y + c)^2}, \quad \theta_1 = \arctan[x/(-y - c)] \tag{6}$$

$$r_2 = \sqrt{x^2 + (y - c)^2}, \quad \theta_2 = \arctan[x/(c - y)] \tag{7}$$

2.2   The Optimization Method of Fracture Spacing

For the reservoirs with natural fractures, the new fractures can communicate with natural fractures to effectively increase the volume of reservoir reconstruction. However, for tight sandstone reservoirs where natural fractures do not develop, when new compression fractures are affected by the induced stress field, complex fractures cannot be formed, and the total fracture propagation length is affected. Therefore, in tight sandstone reservoirs where natural fractures do not develop, the influence of fracture induced stress should be avoided as much as possible [9].

According to the principle of stress superposition, we superimpose the induced stress fields in all directions, if the condition of $\sigma_{x\,min} + \sigma_{xi} > \sigma_{y\,min} + \sigma_{yi}$ is satisfied. That is $\sigma_{xi} - \sigma_{yi} > \sigma_{x\,min} - \sigma_{y\,min}$, the geostress field is redirected, and the new fractures will divert when they expand, instead of following the direction of the initial maximum principal stress, but extending in a direction parallel to the wellbore. There is a certain range of maximum horizontal principal stress reversal and turning areas along the wellbore at different locations on the pre-compression fracture. When the new compression fracture expands outside the maximum horizontal principal stress zone, the fracture still expands in the direction of the original maximum principal stress and is not Effect of induced stress field caused by pre-compression fracture (Fig. 2).
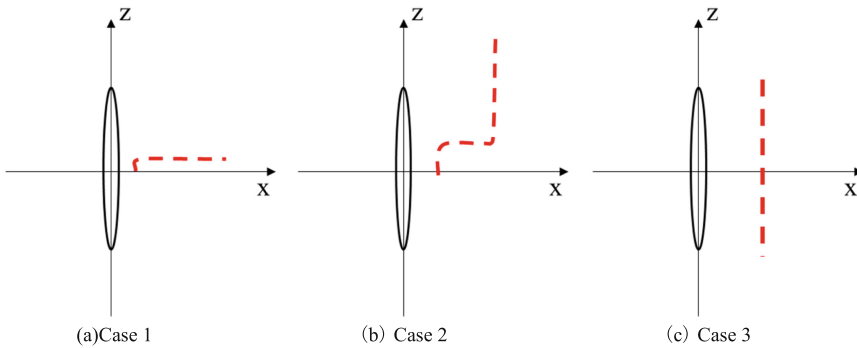

(a)Case 1   (b) Case 2   (c) Case 3

Fig. 2. Schematic diagram of fracture propagation under different conditions

It is considered that under the effect of induce stress, there is a critical cluster spacing (ΔL_{min}) for fracture reorientation which can make the principle stress inverse between clusters. During fracturing design, if the fracture spacing is greater than ΔL_{min}, it can ensure that the propagation of new fractures is basically not affected by the stress induced by pre-fractures.

2.3   Extended Finite Element Method

The XFEM is to introduce two local enhancement functions (step enhancement function and asymptotic crack tip function) to reflect the discontinuity of the fracture surface without changing the calculation grid structure.

$$H(x) = sign(\varphi(x)) = \begin{cases} 1 & \varphi(x) > 0 \\ -1 & \varphi(x) < 0 \end{cases} \tag{8}$$

$$F_\alpha(x) = [\sqrt{r}\sin\tfrac{\theta}{2}, \sqrt{r}\cos\tfrac{\theta}{2}, \sqrt{r}\sin\theta\sin\tfrac{\theta}{2}, \sqrt{r}\sin\tfrac{\theta}{2}\cos\tfrac{\theta}{2}]$$
$$\alpha = 1, 2, 3, 4 \tag{9}$$

Where $H(x)$ is used to characterize the discontinuous displacement field, and $F_\alpha(x)$ is used to characterize the singular displacement field.

The interpolation form of displacement field and pressure field based on XFEM is shown below:

$$\mathbf{u} = \sum_{I=1}^{N} N_I(x)[\mathbf{u}_I + H(x)\mathbf{a_I} + \sum_{\alpha=1}^{4} F_\alpha(x)\mathbf{b}_I^\alpha] \tag{10}$$

$$p = \sum_{I=1}^{N} N_I(x)[p_I + \varphi(x)\mathrm{p_I} + \sum_{\alpha=1}^{4} P_\alpha(x)\mathrm{p}_I^\alpha] \tag{11}$$

In the above formula, N represents the set of all ordinary nodes, $\mathbf{u}_I$ is the conventional node degree of freedom, that is, the displacement of the node; $N_I(x)$ is the standard finite element shape function of the corresponding node; $\mathbf{a_I}$ and $\mathbf{b}_I^\alpha$ are the extended degrees of freedom of the node displacement, $\mathrm{p_I}$ and P_I^α are nodal pressure expansion degrees of freedom; $\varphi(x)$ and $P_\alpha(x)$ are enhanced functions of pressure nodes.

When using the XFEM in ABAQUS for hydraulic fracture propagation simulation, the fracture initiation and propagation adopt the tensile-separation criterion based on the cohesive element damage mechanics. Among them, the constitutive relationship of the rock before damage is linear elasticity. After the element starts to damage, the stiffness gradually degrades until it completely fails. In numerical simulation, the maximum principal stress criterion is used as the crack initiation criterion for hydraulic fractures, that is,

$$f = \frac{\sigma_{\max}}{\sigma_{\max}^c} \tag{12}$$

Where $\sigma_{\max}^c$ is the maximum critical stress to the rock, MPa; $\sigma_{\max}$ is the maximum principal stress to the rock, MPa;

2.4   Basic Assumptions and Conditions for Numerical Simulation

Taking the tight sandstone reservoir in the northern Songliao Basin as an example, the extended finite element method in the ABAQUS platform is used to establish a two-dimensional fracture propagation model. The model geomechanics and fracturing construction simulation parameters are shown in Table 1. The size of the geometric model is 100 * 50 m, the model grid is divided by an unstructured grid. The initial perforation point of the fracture is vertical to the horizontal wellbore. The schematic diagram of the model is shown below (Fig. 3).

Table 1. Basic parameters for numerical simulation.

Modeling parameters	Unit	Value
Young's modulus	GPa	19
Poisson's ratio	\	0.21
Permeability	mD	1.16
Initial porosity	%	12.6
Rock initial pore pressure	MPa	18.5
Tensile strength of rock	MPa	6
Fracturing fluid viscosity	Pa·s	0.001
Filtration coefficient	m/Pa·s	1e−14
Fracturing fluid injection rate	m^3/min	0.2
Minimum horizontal principal stress	MPa	24.4
Maximum horizontal principal stress	MPa	28
Vertical principal stress	MPa	35
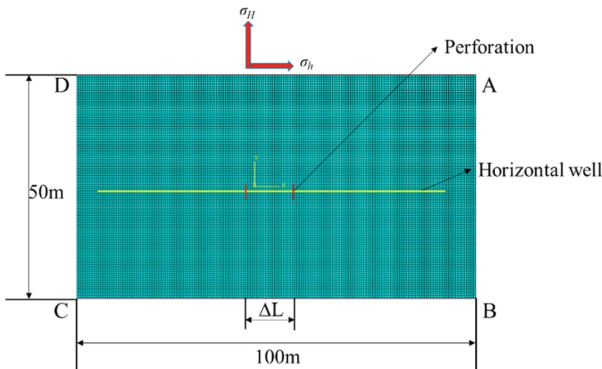
Fig. 3. Schematic diagram of facture spacing optimization model.

3   Numerical Calculation Results and Discussion

3.1   Local Stress Disturbance of Fracture

Figures 4 and 5 show the maximum and minimum principal stress cloud diagrams after the fractures are formed, the horizontal brown line is the horizontal wellbore, and the vertical black line is the hydraulic fracture. It can be seen from the figure that the range of reservoir stress disturbance is mainly concentrated around the smaller sides of the artificial fracture, and at the same time, the stress concentration effect is produced at the artificial fracture tip. After fracturing, the maximum horizontal principal stress direction stress can reach 29.86 MPa, which is an increase of 1.86 MPa from the original maximum principal stress of 28 MPa; the minimum horizontal principal stress direction stress can reach 27.41 MPa, which is an increase of 3.01 MPa from the original maximum principal stress of 24.4 MPa. Regardless of the direction of the maximum

principal stress or the minimum principal stress, the induced stress value in each direction appears to decrease with increasing distance from the fracture, and tends to the original ground stress value at a certain position.

With the fracture initiation point as the origin along the wellbore direction of the horizontal well, the relationship diagram of induced stress at different distances from the pre-pressed fracture is drawn. Analysis of Fig. 6 shows that the disturbance of the minimum horizontal principal stress of the fracture is more significant. The induced stress decreases gradually with the horizontal distance from the fracture, and decreases to 0 at about 20m from the fracture, which is the same as the original geostress state.
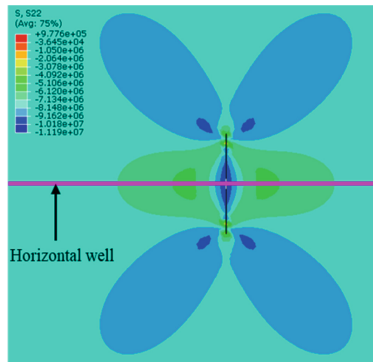

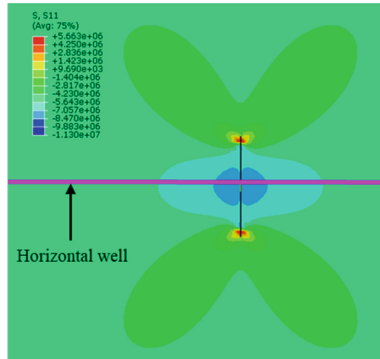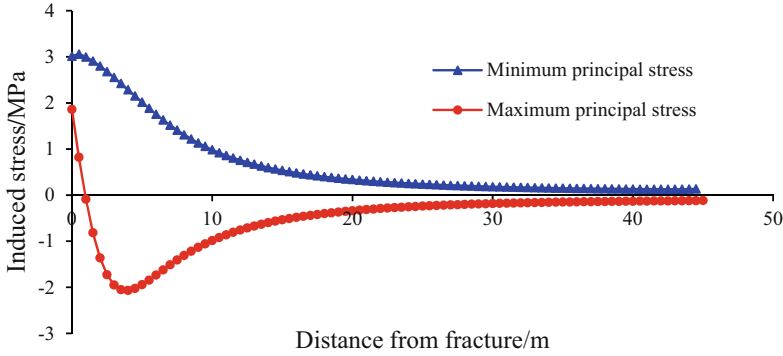**Fig. 4.** Maximum principal stress distribution.

Fig. 5. Minimum principal stress distribution

Fig. 6. Diagram of induced stress at different distances from pre-pressed fractures

Based on the data of Fig. 6 defined by the induced stress difference, the calculated induced stress difference at different distances from the fracture is calculated as shown in Fig. 7. Figure 7 shows that the induced stress difference increases first and then decreases along the direction of the wellbore, and finally decreases to 0 at a place far from the fracture. The maximum induced stress difference of 4.6 MPa is greater than the initial horizontal ground stress difference of 3.6 MPa. According to the previous theoretical analysis, the direction of the maximum horizontal principal stress has been reversed in the area where the induced stress difference is greater than the original horizontal stress difference. When a new fracture expands in this area, the fracture direction will follow the horizontal wellbore direction. Therefore, the position where the induced stress difference is equal to the original in-situ stress difference is defined as the minimum cluster spacing $\Delta Lmin$.
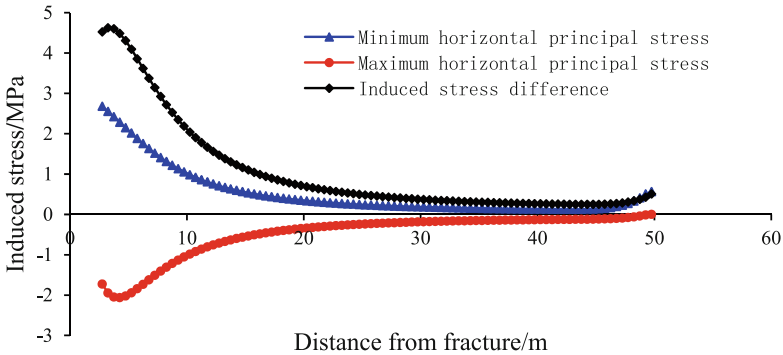
Fig. 7. Diagram of induced stress at different distances from pre-pressed fractures

Calculate the induced stress difference at different positions in the direction of the fracture height of the pre-compressed fracture, compare it with the original horizontal ground stress difference, and draw the ground stress reversal zone $\Delta\sigma_i > \Delta\sigma_0$ and the ground stress turning zone $0 < \Delta\sigma_i < \Delta\sigma_0$ (Fig. 8), It is calculated that the point where the boundary of the stress reversal area intersects with the horizontal wellbore is about 6.5 m from the pre-pressed fracture (ΔLmin = 6.5 m). It is not necessary to arrange a second fracture within the range of 6.5 m from the pre-pressed fracture.
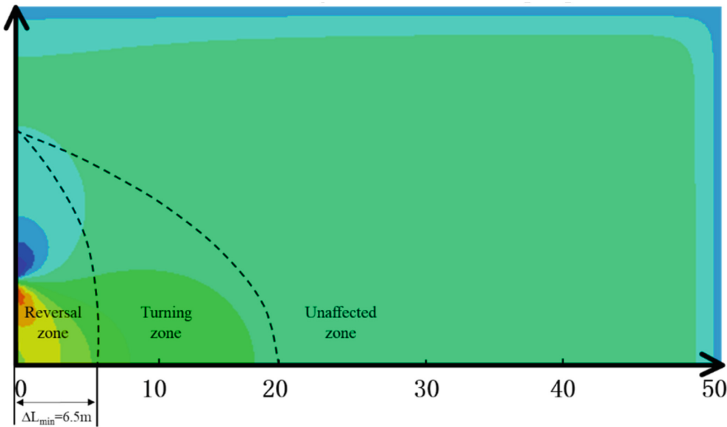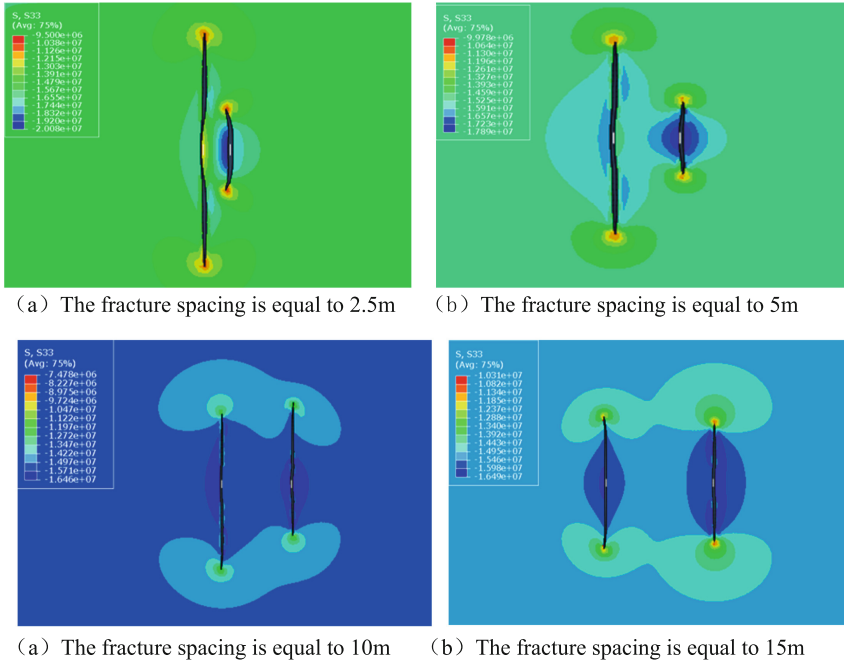

Fig. 8. Schematic diagram of stress interference area around a single fracture

3.2   Optimization Results of Fracture Spacing

Take single fractures as an example to verify the accuracy of the division of the stress redirection area; set the fracture spacing to 2.5, 5, 10, and 15 m respectively for simulation. When the fracture spacing is equal to 2.5 and 5 m (Fig. 9a and Fig. 9b), the fracture propagation is seriously affected by the stress interference of the pre-press crack, the fracture is distorted, the size is small, and it is difficult to form effective fractures. When the fracture spacing is equal to 10 and 15 m (Fig. 9c and Fig. 9d), the post-fracture is less disturbed by stress, the size of the post-fracture is similar to the shape of the first-fracture.

（a）The fracture spacing is equal to 2.5m   （b）The fracture spacing is equal to 5m

（a）The fracture spacing is equal to 10m   （b）The fracture spacing is equal to 15m
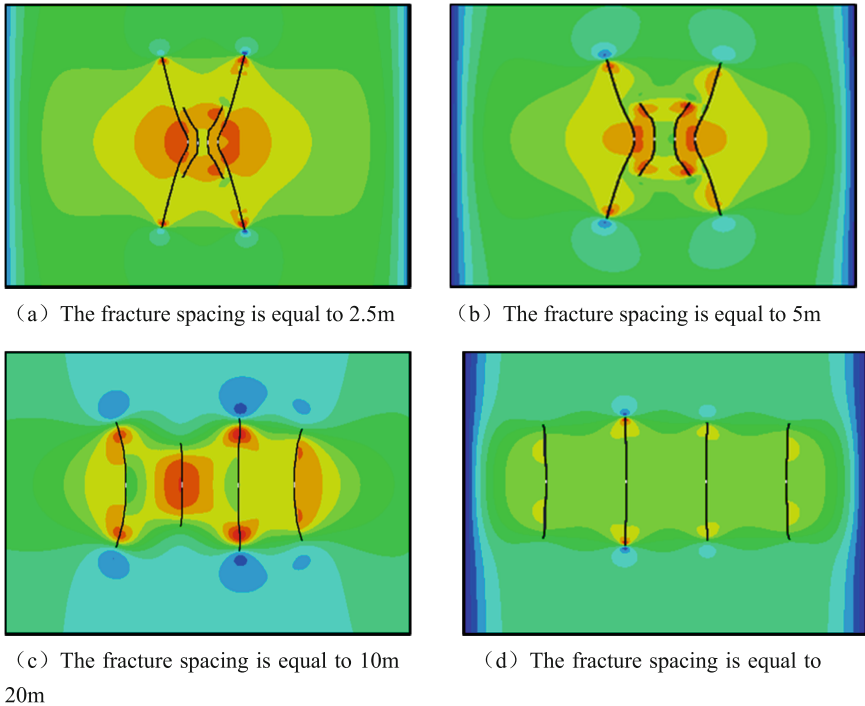
Fig. 9. Schematic diagram of fracture propagation at different fracture spacings

In the process of multi-cluster perforation fracturing, multiple fractures will extend simultaneously. Based on the analysis of the stress interference of the two fractures, taking multiple fractures as an example to verify the accuracy of the division of the stress redirection area; set the fracture spacing to 2.5, 5, 10, and 20 m respectively for simulation. When the fracture spacing is equal to 2.5 and 5 m (Fig. 10a and Fig. 10b), that is, new fractures are arranged in the reversal zone, and the results show that the new compression fractures are severely affected by the stress interference of the pre-compression fractures, and the intermediate fracture expansion size is small. The total fracture length is significantly affected and it is difficult to form an effective fracture. When the crack spacing is equal to 10 m (Fig. 10c), that is, the new crack initiates in the stress turning zone. The results show that the crack propagation process is affected by the composite stress, and the intermediate crack extension length is slightly limited; When the fracture spacing is equal to 20 m (Fig. 10d), the fractures are affected by stress interference very little, and each fracture can independently expand, forming an artificial main fracture parallel to the previous fracture and equal in size.

For the dense cutting fracturing technology, the output is positively related to the number of fractures. When fracturing design is performed, it is necessary to minimize the fracture spacing while ensuring that each fracture can form an effective artificial main fracture. From the results of numerical simulation verification, the arrangement of fracture spacing cannot be less than the minimum cluster spacing $\Delta Lmin$. Based on this principle, the arrangement of fracture spacing is used to complete the fracture

arrangement of all horizontal well sections. In actual engineering applications, due to the complex geological conditions of the reservoir, cementing quality, and fracturing timing, factors such as comprehensive calculation and consideration are required to complete the optimization of fracture spacing.

（a）The fracture spacing is equal to 2.5m   （b）The fracture spacing is equal to 5m

（c）The fracture spacing is equal to 10m   （d）The fracture spacing is equal to
20m

Fig. 10. Schematic diagram of fracture propagation at different fracture spacings

4   Conclusion

(1) The range of the induced stress field generated by the pre-pressing fracture is concentrated in a small area around the fracture. As the distance from the pre-pressing fracture increases, the induced stress difference increases first and then decreases.There is a horizontal principal stress reversal zone and a turning zone around the pre-compressed fracture.

(2) Define the horizontal distance between the pre-fractured fracture and the point where the boundary of the stress reversal zone intersects the horizontal wellbore as the minimum cluster spacing ΔL_{min}. When the fracture spacing is less than ΔL_{min}, the new fractures cannot be effectively fractured due to the induced stress field generated by the pre-fracture. This can be used as the principle for determining the minimum fracture spacing of the dense cutting fracture technology.

(3) According to the tight sandstone reservoir conditions in the northern Songliao Basin, using the established fracture spacing optimization method to optimize the minimum cluster spacing of 6.5–10 m. The simulation results show that when the fracture spacing is greater than ΔL_{min}, the newly-compressed fracture is basically not affected by the induced stress field generated by the pre-compressed fracture, and finally multiple fractures are formed in the reservoir.

References

1. Sun, L., Zou, C., Jia, A., et al.: Development characteristics and orientation of tight oil and gas in China. Petrol. Explor. Dev. **46**(6), 1015–1026 (2019)
2. Zou, C., Zhu, R., Bai, B., et al.: Significance, geologic characteristics, resource potential and future challenges of tight oil and shale oil. Bull. Mineral. Petrol. Geochem. **34**(1), 3–17 (2015)
3. Jia, C., Zou, C., Li, J., Li, D., Zheng, M.: Assessment criteria, main types, basic features and resource prospects of the tight oil in China. Acta Petrolei Sinica **33**(3), 343–350 (2012)
4. Cui, M., Liu, Y., Xiu, N., et al.: Analysis of factors affecting the formation of Effective Stimulated Reservoir Volume (ESRV). Oil Drill. Prod. Technol. **36**(02), 82–87 (2014)
5. Zhang, S., Guo, T., Zhou, T., et al.: Fracture propagation mechanism experiment of hydraulic fracturing in natural shale. Acta Petrolei Sinica **35**(03), 496–503+518 (2014)
6. Zhang, Y., Pan, L., Zhou, T., et al.: A study of hydraulic fracture propagation for shale fracturing. Sci. Technol. Eng. **15**(5) (2015)
7. Jin, C., Yang, D., Zhang, Y., et al.: Optimization techniques for stimulation design of horizontal wells of Heterogeneous tight oil in northern Songliao Basin. China Petrol. Exp. **19**(6), 40–46 (2014)
8. Lin, T., Kang, D., Jiang, L.: Geological characteristics and exploration potential of the tight oil in Fuyu oil reservoirs of North Songliao Basin. Petrol. Geol. Oilfield Develop. Daqing **38**(05), 94–100 (2019)
9. Mu, L., Zhao, Z., Li, X., et al.: Fracturing technology of stimulated reservoir volume with subdivision cutting for shale oil horizontal wells in Ordos Basin. Oil Gas Geol. **40**(3), 626–635 (2019)
10. Mayerhofer, M.J., Lolon, E., Warpinski, N.R., Cipolla, C.L., Walser, D.W., Rightmire, C. M.: What Is Stimulated Reservoir Volume? Society of Petroleum Engineers, 1 February 2010. https://doi.org/10.2118/119890-PA
11. Cipolla, C.L., Warpinski, N.R., Mayerhofer, M., Lolon, E.P., Vincent, M.: The Relationship Between Fracture Complexity, Reservoir Properties, and Fracture-Treatment Design. Society of Petroleum Engineers, 1 November 2010. https://doi.org/10.2118/115769-PA.
12. Xu, J., Li, J., Wu, Y., et al.: Exploration and practice of volume fracturing technology in horizontal well of Mahu tight conglomerate reservoirs. China Petrol. Exp. **24**(2), 241–249 (2019)
13. Tang, R., Wen, Q., Su, J., et al.: Factors affecting productivity of stage fractured horizontal well. Petrol. Drilling Tech. **38**(2), 80–83 (2010)
14. Gao, H., Cheng, L., Qu, Z.: Optimization of the fracture parameters of fractured horizontal wells. Jo. Xi'Shiyou Univ. **21**(2), 29–32 (2006). Natural Science Edition

15. Bunger, A.P., Zhang, X., Jeffer, Y.R.G.: Parameters affecting the interaction among closely spaced hydraulic fractures. SPE 140426 (2011)
16. Green, A.E., Sneddon, I.N.: The distribution of stress in the neighbourhood of a flat elliptical crack in an elastic solid. Math. Proc. Camb. Philos. Soc. **46**(1), 159–163 (1950)
17. Sneddon, I.N.: The distribution of stress in the neighbourhood of acrack in an elastic solid. Proc. R. Soc. Lond. Ser. A **187**, 229–260 (1946)
18. Sneddon, I.N., Elliott, H.A.: The opening of a Griffith crack under internal pressure. Q. Appl. Math. **3**, 262–267 (1946)